Soil Loss and Sediment Yield Prediction in Lake Hawassa Sub-Basin, Central Rift Valley Basin, Ethiopia

Authors: Gebre, Agegnehu Mitiku, Belete, Mulugeta Dadi, and Belayneh, Moltot Zewdie

Source: Air, Soil and Water Research, 17(1)

Published By: SAGE Publishing

URL: https://doi.org/10.1177/11786221241261823

Soil Loss and Sediment Yield Prediction in Lake Hawassa Sub-Basin, Central Rift Valley Basin, Ethiopia

Air, Soil and Water Research
Volume 17: 1–18

DOI: 10.1177/11786221241261823

Agegnehu Mitiku Gebre[1], Mulugeta Dadi Belete[1] and Moltot Zewdie Belayneh[1]

[1]Hawassa University Institute of Technology, Ethiopia

ABSTRACT: For effective water and land resource management in data-scarce areas, it is imperative to investigate the spatial variability of sediment yield using a rapid, reliable, and affordable approach. The current study demonstrated the use of tools and models viz. Geographic Information System (GIS), Revised Universal Soil Loss Equation (RUSLE), and Sediment Delivery Ratio (SDR) based approach for the assessment of soil loss and sediment yield rate in Lake Hawassa Sub-basin. Input data used were soil, rainfall, digital elevation model (DEM), and land use and land cover change (LULC) maps. The result of the study showed that there was significant and widespread soil loss and sediment yield on cultivated land dominated by moderate, steep and very steep slopes with little vegetation and barren areas. An estimated mean of 16.36 t/ha/year, or 1.97 million tonnes of soil is lost annually by sheet and rill erosion across the Sub-basin. The sediment delivery ratio (SDR) at the outlet of the lake sub-basin was 0.249. Accordingly, the quantified sediment yield at the sub-basin outlet, taking into account the average-based soil loss and sediment delivery ratio, was found to be 4.07 t/ha/year. The annual siltation rate of the lake from these two forms of erosion was found to be 1.01 cm/year. Therefore, depending on the severity of the soil loss, appropriate Best Management Practices (BMP) should be applied to reduce the rate of soil loss and sediment yield to protect the lake and its ecosystem.

KEYWORDS: RUSLE, SDR, GIS, soil loss, sediment yield

RECEIVED: February 23, 2024. **ACCEPTED:** May 28, 2024.

TYPE: Original Research

CORRESPONDING AUTHOR: Agegnehu Mitiku Gebre, Hawassa University Institute of Technology, P.O. B. 05 Hawassa, Ethiopia. Email: agegnehumitiku4@gmail.com

Introduction

The dynamic evolution of soil erosion results in detached, transported, and off-sediment, impacting landforms, geomorphic processes, and changes in sediment fluxes in rivers and Lake Watersheds (T. G. Abebe & Woldemariam, 2024; Aga et al., 2018, 2019; Ebabu et al., 2019; Sabri et al., 2017; Yesuph & Dagnew, 2019). Approximately 46% land degradation of the worldwide is contributed by water erosion (den Biggelaar et al., 2003) and is responsible for 15 to 30 billion tons of the yearly sediment taken by the world's water erosion to reservoirs and lakes (Thomas et al., 2018).

In Ethiopia, soil loss due to water is a significant issue with negative consequences on hydroecology and crop production, resulting in economic loss, reservoir sedimentation, and downstream flooding (Gebrehiwot et al., 2014; Haregeweyn et al., 2015, 2016). Lake Hawassa Sub basin, there is considerable erosion and sedimentation caused by human activities such as rapid land use/cover change, sand mining, declining of forest cover, farming on hilly topography and urban expansion (Y. Abebe et al., 2018; Belete et al., 2021; Degife et al., 2019; Gebre et al., 2023; Kassay et al., 2023; Moges & Holden, 2008). The eroded sediments usually end up in the lake from all directions in the watershed (Y. Abebe et al., 2018; Degife et al., 2019; Gebre et al., 2023; Tsegaye & Bharti, 2022).

Soil conservation planning and water management strategy implementation essentially require an accurate quantification of the soil erosion rate from watersheds as well as sediment deposition in such dynamic watersheds (Asare & Boye, 2021; Camacho-Zorogast et al., 2023; Dinka, 2020). However, predicting soil loss is challenging because of the difficulty in determining the factors that cause it (Awulachew et al., 2017; Leta et al., 2023; Tsegaye & Bharti, 2022) modelling the processes driving soil loss and silt deposition helps advance our understanding of the issues affecting the entire basin in relation to the crucial elements influencing soil loss and the associated sediment transportation (Awulachew et al., 2017; Endalew & Biru, 2023). Thus, predicting the sediment loading rate and sediment production of a given watershed, estimation of soil loss rates, and sediment delivery ratios using geospatial data is essential and useful in areas that have scarce observed sediment data. This plays an important role in stakeholder decision-makers' ability to plan strategic catchment management interventions to adopt soil and water protection actions in hotspot areas to prevent land degradation (Bekele & Gemi, 2021; Belay et al., 2020; Yusof et al., 2023).

Numerous models have been developed for soil loss and sediment yield prediction, including simple empirical models such as the universal soil loss equation (USLE; Wischmeier & Smith, 1978) and revised version universal soil loss equation (RUSLE; Renard et al., 1997), and very complicated models such as European Soil Erosion Model (EUROSEM; Dinka, 2020) and Soil Water Assessment Tool (SWAT; Arnold et al., 2007). However, these models typically require a large amount

of data; thus, their application is limited to data-scarce regions (Wang et al., 2013).

An empirical soil loss prediction model, such as the Revised Universal Soil Loss (RUSLE) model, is the most extensively applicable and accepted model for soil erosion assessment and has been used in numerous studies (Erol et al., 2015; Kulimushi et al., 2021; Kumar & Singh, 2021; Panditharathne et al., 2019; Yusof et al., 2023). It has been extensively used to determine sheet and rill soil erosion and the design of soil loss control and regulating measures for cultivated, barren, and grassland (Panditharathne et al., 2019). Moreover, it is adaptable, cost-, and time-effective with the ability to estimate soil loss with limited data, which is particularly useful in developing countries (Angima et al., 2003; Camacho-Zorogast et al., 2023; Renard et al., 1991). However, the RUSLE model cannot predict whether the sediment will be exported or re-deposited within the watershed because colluvium or alluvium is its limitation (Hui et al., 2010). Therefore, it is essential to introduce a stream channel slope-based sediment delivery ratio (SDR) model when calculating the sediment production of a given catchment to correct the higher erosion rates produced by the RUSLE model for its reduction effect (Mutua & Klik, 2006). Thus, SDR measures the effectiveness of sediment delivery to confidante the quantity of soil actually conveyed from the erosion source point of a watershed exit to the gross quantity of soil loss detached from the same watershed upstairs at that point (Mutua & Klik, 2006).

Consequently, different SDR relationships have been developed with combinations of catchment physical features, such as landscape gradient and its length ratio, land-use types, drainage area, runoff rainfall factors, and sediment unit mass (Leta et al., 2023; Ouyang & Bartholic, 1997). Among the several SDR techniques, Williams and Berndt's technique of estimating the SDR yields operative results in cases where data are scarce (Gelagay & Minale, 2016; Kidane et al., 2019; Onyando et al., 2005; Panditharathne et al., 2019; Williams & Berndt, 1977). This method can be used to ascertain how topographical factors, such as stream length and stream height ratio, influence sediment transport within a watershed. In addition, the RUSLE model was found to be more accurate when combined with GIS, RS, and SDR models, which also helps address the sediment yield of the given watersheds (Haregeweyn et al., 2017; Tsegaye & Bharti, 2022). Therefore, in order to address the above issues, the objective of the study is to estimate the soil erosion and sediment in the Lake Hawassa sub-basin.

Description of the Study Area

The Hawassa Lake sub-basin is a closed system with a total area of 1,366.65 km^2 and is located in the central north-eastern part of the Rift Valley Lakes Basin of Ethiopia (Gebre et al., 2023). The lake sub-basin is divided into ten small sub-basins for low level watershed management based on their expected contribution to soil loss and sediment yield. This classification

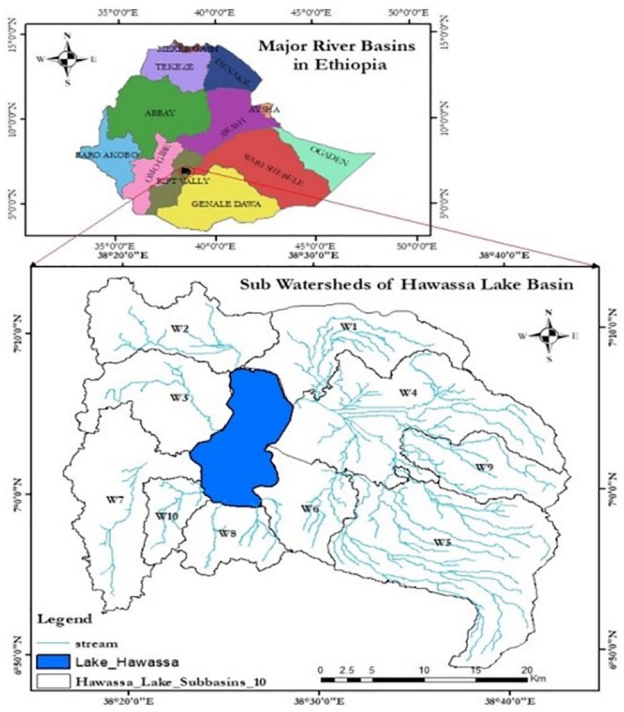

Figure 1. Study area map.

is based on the fact that all ten sub-basin catchments have their own inlet drainage system into Lake Hawassa, the representative sediment yield prediction is more reliable in such a drainage system. The geographical location is at latitudes 6°48′45′ and 7°14′49″ N and longitudes 38°16′34″ and 38°43′26″ E (Figure 1), with the lowest and highest elevations at 1,624 and 2,987 m.a.s.l. respectively, as shown in Figure 1 (Gebre et al., 2023). The lake sub-basin is characterized by high population growth, with a projected total population of 2,491,295 in 2020, of which 23% is urban (Degife et al., 2021).

Water body, wetland, forest, bush land, shrub land, grass land, built-up land, cultivated land and barren land are the eight LULC types of the lake sub-basin (Degife et al., 2019). The dominant economic activity in the basin was agriculture, which was characterized by subsistence farming with some commercial farming and livestock production (Y. Abebe et al., 2018).

In the lake sub-basin, the Tikur Wuha River is the perennial river that originates from the eastern escarpments. In the western side, the lake sub-basin is affected by gullies, in which the sixteen gullies are active and directly connected to Lake Hawassa (Gebre et al., 2023). Topographically, most of the sub-basin is flat to gently rolling, but bordered by steep escarpments. Altitude ranges from 1,680 m at Lake Hawassa to 2,700 m on the eastern escarpment: an altitude range of 1,020 m. Most slopes (56%) are flat to gentle (0%–8%), with a further 33% moderately steep (8%–30%), and only 5% steep to very steep (>30%) (Belete, 2020; Gebre et al., 2023). The average annual rainfall of the sub-basin is 1,050 mm, rainfall data from meteorological stations (1991–2020) (Gebre et al., 2023).

Table 1. Severity Classification of Soil Loss Adopted from FAO (2006).

SOIL LOSS RATE (T/HA/YEAR)	0–5	5–10	10–25	25–45	>45
Severity classes	Very slight	Slight	Moderate	Severe	Very severe

The geological characteristics and formation of the area are volcanic lacustrine deposits composed of tuff, pumice and ash with the sediments consist of alternating fine and coarse sands with high permeability (Ayenew et al., 2018). The Lake Hawassa sub-basin is dominated by 11 major soil types, of which five are predominant: Andosols (28.57%), Luvisols (26.47%), Fluvisols (26.7%), Leptosols (1.12%), Vertisols (10.71%), and Regosols (5.33%) (Gebre et al., 2023). Furthermore, the soils of the catchment can be classified into four textural classes: sandy loams (including red and grey varieties), silty loams, clays and thin gravelly sand soils (Belete, 2020).

Material and Methods

Prediction Soil Loss and Sediment Yield

Soil Loss by Sheet and Rill Erosion. The annual average soil loss was assessed in the form of rill erosion and sheet by using Geo-informatics and Soil Loss prediction RUSLE model. This was computed using five erosion parameters (equation (1)) (Renard et al., 1997).

$$A = R*K*LS*C*P \quad (1)$$

Where A is mean annual average soil loss (t/ha/year), R is rainfall erosivity (MJ mm/hr/ha/year), K is soil-erodibility (t/ha/MJ/mm), LS is gradient length and gradient, C land-cover management and P land management factors, respectively. After determining the soil erosion, five soil loss severity classes were developed (FAO, 2006) by re-categorizing the erosion map according to the severity class used in several studies, as shown (Table 1).

*Erosivity (*R*) Factor.* It is the capability of rainfall to remove and transport detached materials in a specific area, and the RUSLE model uses this factor as input in soil loss determination (Hategekimana et al., 2020). This factor can be estimated as a function of kinetic-energy/rain drop/and their 30-minute maximum intensity (I_{30}) (Renard et al., 1997). However, measurements to generate these variables are not available for Ethiopia as a whole. Therefore, the equation developed by Hurni (1985) was applied to relate R to the annual rainfall in different parts of Ethiopia (equation (2)).

$$R = P * 0.562 - 8.12 \quad (2)$$

Where R (erosivity factor) (MJ mm/ha/hr/year) and P is the annual average daily rainfall (mm). The 30 years (1991–2020) data of the daily rainfall (P) of five stations were obtained from the Ethiopia Metrological Agency (EMA). The determined R value was interposed using the inverse distance weight (IDW) technique (Kulimushi et al., 2021; Panditharathne et al., 2019) to develop spatial values. This technique is preferred to the geo-arithmetic spatial interpolation method because it is easy to produce comparatively correct evidence of precipitation erosivity from identified sample points to points of unidentified values at a short distance. It also gives reliability of erosivity values over the entire surface and gives minimal error (Panditharathne et al., 2019). Thus, this erosivity factor (R) map was prepared with a grid size of 30 × 30 m in Arc GIS 10.7 environments by using five station rainfall data obtained from ENA.

*Erodibility (*K*) Factor.* It is an indicator of the impact of soil properties on soil loss and the vulnerability of soil to erosion (Renard et al., 1997). To determine the K-factor in this study, the method developed in Hurni (1985) for a data-scarce region was adopted. Collection of representative data in the largest area is difficult, and the K (expressed in t/ha/hr//MJ/ha/mm) values (for this specific investigation were determined from the soil unit type of the study area as obtained from the harmonized world soil database (HWSD) with a spatial resolution of 250 × 250 m (FAO, 2015). The soil erodibility layer of the sub-basin with a grid size of 30 m was generated using ArcGIS software version 10.7.

*Slope Length—Steepness (*LS*) Factor.* It describes the impact of the local landscape on the rate of soil loss (Nyesheja et al., 2019). The steepness gradient affects the flow velocity, whereas the gradient length identifies the distance between the points where erosion begins and the deposition (Renard et al., 1997) presented in equation (3) was used (Moore & Burch, 1986).

$$LS = \left(Flow\ Accumulation * \frac{Cell\ size}{22.13} \right)^{N} * \left(\frac{sins\ lope}{0.0896} \right)^{M} \quad (3)$$

Where N = 0.4 and M = 1.3 were utilized for the purpose of the study, the values provided by Moore and Burch (1986). The flow direction, flow accumulation and gradient along with unit river power erosion and sink procedures were calculated using input of 30 × 30 m resolution DEM in the hydrological extensions of "Spatial Analyst Tool Surface Slope Map Algebra Raster Calculator" in the ArcGIS 10.7.

*Land Covers Management (*C*) Factor.* The cumulative effects of trees, agricultural sequences, and other land cover conditions on land degradation were quantified by land cover management (C-Factor; Molla & Sisheber, 2017; Wischmeier & Smith, 1978). The land use land cover (LULC) data, which indicate the current situation of the study area (Karaburun, 2010; Tikuye et al., 2023). The Random forest based land

use and land cover classification approach was used because it is an effective way of classifying land cover because it uses a large number of decision trees to produce reliable results. It can also handle large datasets and can be used to produce accurate results quickly (Tikuye et al., 2023). These data were allocated based on the classified map and distributed among various LULC forms. The *C*-factor values ranged from 1 for bare land to 1/100 for forest (Neitsch et al., 2009). The map was produced using the ERDAS Imagine INE 2014 software (under supervised land cover classification) using the input of 2020. Landsat 8 OLI image with 30 m resolution were obtained from the Earth Explorer (EE) database (https://earthexplorer.usgs.gov) of the United States Geological Survey (2022). After similar characteristics were reviewed, *C*-factor values were allocated to the LULC conditions in the study watershed and modified in raster formats in the GIS Environment (Hurni, 1985). Finally, the accuracy of the supervised classification was determined by a confusion matrix using the kappa coefficient, user, producer, and overall accuracy, and the LULC group of the Lake sub-basin *C*-factor map was generated.

*Conservation-Provision Practice (*P*) Factor.* The conservation support factor component can be determined by the type of soil erosion protection practices used in the field, such as terracing, strip cropping, and contour cultivation, which are the three most well-known interventions for enhanced soil and water conservation in agricultural areas (Renard et al., 1997). However, these conservation practices in this particular area are not properly implemented, and some are damaged owing to a lack of continuation (Dinka & Klik, 2019; Endalew & Biru, 2023). Owing to these and related issues, numerous studies have excluded support practice elements from analysis because they are challenging to precisely determine (Renard et al., 1997). Alternatively, the *P* factor can be determined using Wischmeier and Smith (1978) approach, and the *P*-factor values were adopted from the literature by further subdividing the study sub-basin into cultivated land and other land use types. According to Wischmeier and Smith (1978), the support practice (*P*) component, which is combined with non-cultivated lands, can vary from 0 to 1 and can be determined for cultivated lands of different slope classes. Cultivated land was additionally considered the six slope-categorized; land management actions are reliant on slope-groups. As a result, the land-uses/covers of this investigation sub-basin were divided into cultivated and other lands to establish the *P*-factor components of the Lake sub-basin using the LULC map and overlaying percent map showing the matched gradient using the reclassification approach in ArcGIS 10.7, and finally, the *P* factor map was produced.

Sediment Delivery Ratio/SDR/Determination. Numerous sediment delivery ratio (SDR) relationships have been developed based on combining the variable physical characteristics of a catchment (Leta et al., 2023; Williams & Berndt, 1977) however, their application is limited to small catchments with adequate data (Mutua & Klik, 2006). Therefore, the computing of sediment yield without adequate sediment data is an effective approach to accurately estimate the SDR and has been recommended (Camacho-Zorogast et al., 2023; Gelagay & Minale, 2016; Kidane et al., 2019; Onyando et al., 2005; Panditharathne et al., 2019; Wagari et al., 2024). Therefore, the empirical equation (4) by Ouyang and Bartholic (1997) was used in this study by considering the gradient in the main river network to calculate the SDR in the case of inadequate sediment data and mathematically:

$$SDRi = 0.627 * \left(SLPi\right)^{0.403} \tag{4}$$

Where, SLP*i* is percent gradient of in *i*th river network.

For this purpose, the DEM data was adjusted for basin, stream networks course, flow accumulation and river channel was decided using the Arc-GIS 10.7 extension of Arc Hydro Tools. By using the output drainage line and raw DEM, the average main stream network gradient (SLP) value in percentage for each cell in the flow line was calculated to estimate the SDR value for the upper tributary of the cell. Subsequently, the SDR for each cell in the flow channel was calculated using a raster calculator (map algebra extension) in ArcGIS 10.7 (Hui et al., 2010).

Sediment Yield (SY) Estimation. Gross erosion and sediment delivery ratio are two inputs that affect sediment yield. Due to the fact that these parameters cannot be measured directly and that there are no sediment measurement sites in the study area or nearby, including the outlet of the study lake, these variables were used to estimate the SY as used in several previous studies (Endalew & Biru, 2023; Gelagay & Minale, 2016; Kidane et al., 2019; Onyando et al., 2005; Ouyang & Bartholic, 1997; Panditharathne et al., 2019). Sediment yield was calculated by superimposing the sediment delivery ratio and the mean annual soil loss raster layer using the raster calculator geoprocessing tools within the GIS framework of the arc hydro extension tools. Then sediment yield was determined using (equation (5)) (Hui et al., 2010).

$$SY = \sum_{i=1}^{n} SDRi * SL \tag{5}$$

Where *SL* is the quantity of soil loss in the *i*th catchment cell, SDR is the percentage of soil erosion that finally reaches the closest network, and *n* is the total number of cells in the catchment.

The general methodology of the study display below in Figure 2.

Assessment of Land Use Policy Implementation. Because of the tremendous soil erosion that occurs in cultivated lands on steep

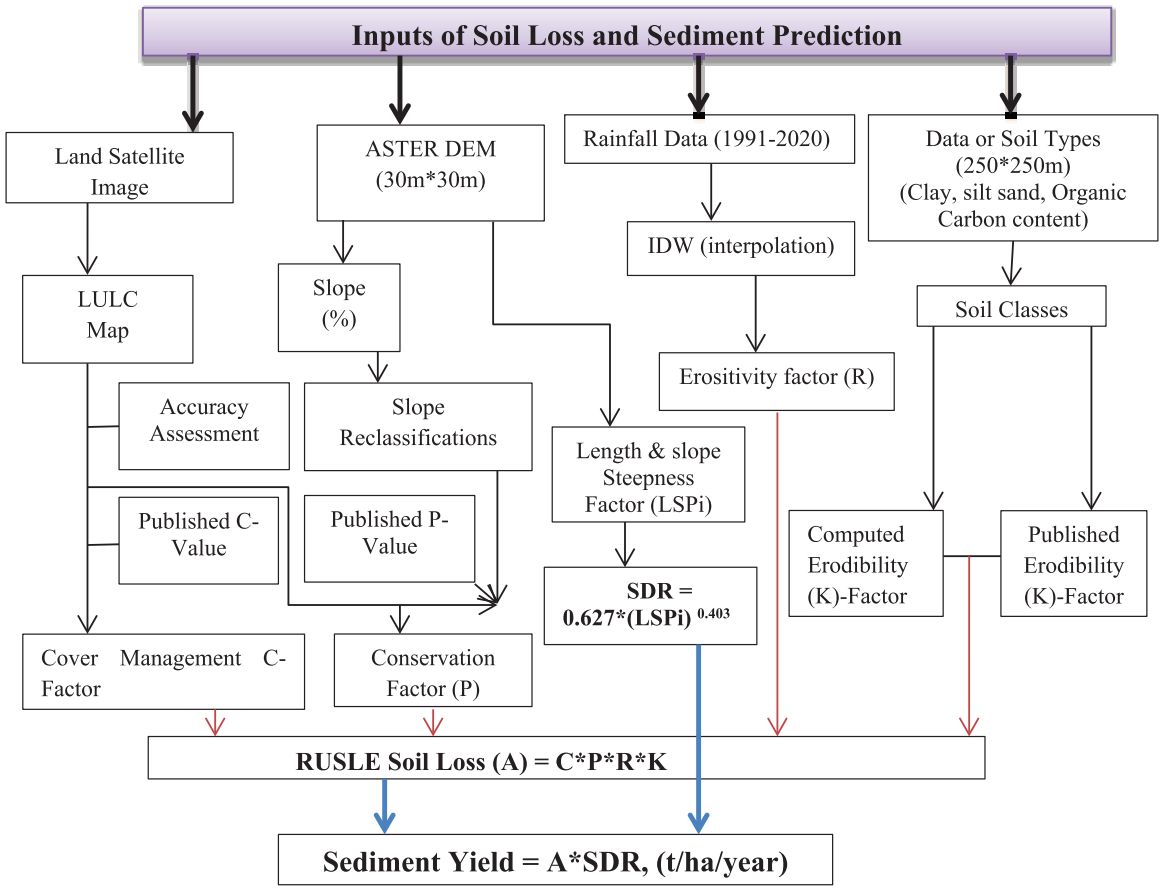

Figure 2. General study methodology flowchart.

slopes, it may be preferable to use these areas for perennial crops or forests (Zhang et al., 2014). River basin strategic plans and land policies in Ethiopia aim to decrease land degradation and production losses (Alemu, 2011). The policy is primarily concerned with land management practices based on the steepness/slopes of the land. According to Ethiopia Rural Land Administration and Land-Use Proclamation No. 456/2005, which was used to classify slopes, land with slopes between 31% and 60% can only be used for annual crops if bench terraces are built, and slopes between 15% and 30% should be seriously considered for SWC techniques. Farming and free grazing were not permitted on slopes greater than 60%. Therefore, using the country's rural land-use policy criteria and the actual state of land use and land cover, the implementation of land-use policy was evaluated in this study (Alemu, 2011) with the support of field observations.

Validation and Consistency of the Model Outputs. Due to the lack of adequate data to compare model estimates with actual soil loss, two alternative approaches were used for validation of the study results. Thus, the first approach is field visit combined with the use of high-resolution images, that is, the accuracy of the RUSLE model in predicting the output of the severity of the soil loss rate in this study was checked field visit. From the field visit, geographic locations of points were collected using a hand GPS and a confusion matrix was carried in a high-resolution satellite image to validate the five soil erosion vulnerability classifications used to designate the soil erosion risk of the study area. In the confusion matrix, the overall, user, and producer accuracy, as well as the kappa coefficient, were determined. At the field visit, observations were made for validation of the model results, according to easily explainable adjustable biophysical features and national level variables. Expert judgement and rating were also incorporated for local and country-wide soil loss rate scoring, specifically by taking into account similar agro-ecological zones found in various regions of Ethiopia, those of the main factors affecting soil erosion, such as topography and climatic setting factors (T. G. Abebe & Woldemariam, 2024; Haregeweyn et al., 2017; Hurni, 2016).

By contrasting it with data from other studies that verified their work using comparable methodologies (Degife et al., 2021; Haregeweyn et al., 2017; Leta et al., 2023; Yesuph & Dagnew, 2019; Zerihun et al., 2018) and the hydrological model-based method suggested by Biondi et al. (2012) were applied to evaluate the consistency and accuracy of the model estimation. Thus, the comparison was made alongside the revisions of other studies conducted in adjacent regions, mostly by similar agro-ecological and climate settings of the areas. Thus, both strategies are equivalent and provide supplementary support for the findings of this study.

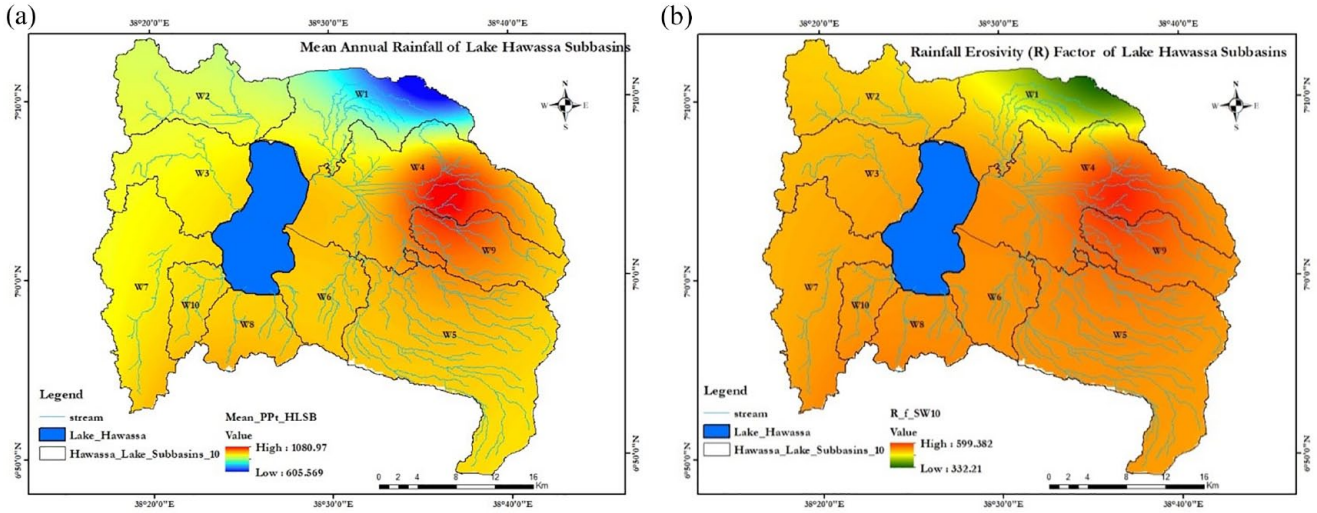

Figure 3. Rainfall (a) and erosivity factor (b) maps of Lake Hawassa watershed.

Table 2. Mean Annual Precipitation (*P*) and Calculated *R*-Factor Values from Different Stations in the Area Studied.

S. NO.	STATION NAME	LAT.	LONG.	ELEV. (M) (M.A.S.L,)	*P* (MM)	*R*-FACTOR (MJ MM HA/ HR/YEAR)	AREA COVERAGE	
							IN KM²	IN %
1	Hassawita	38.56º	6.9º	2,267	1,099	607.26	218.39	15.98
2	Yirbaduwancho	38.03º	6.93º	2,023	1,023	564.93	275.65	20.17
3	Wondo-Genet	38.62º	7.08º	1,742	1,236	683.85	279.21	20.43
4	Shashemene	38.6º	7.20º	1,927	810	445.27	90.88	6.65
5	Hawassa	38.48º	7.07º	1,694	958	528.26	502.52	36.77

Note. The mean and standard deviation of the annual erosivity factors (*R*) at each meteorological station were found to be 523.03 and 85.68 MJ mm/ha/hr/year, with ranges from 445.27 to 688.03 MJ mm/ha/hr/year.

Results

Estimation of RUSLE Input Factor

*Rainfall-Erosivity Factor (*R*).* The spatial distribution of the erosivity factor (*R*) over the study area is shown in Figure 3b and its values are given in Table 2. Thus, the *R* values of the lake catchment were determined from five rainfall stations. The annual rainfall of a long period of time ranged from 605.56 to 1,080.97 mm, with the standard deviation and mean values of 153 and 1,060 mm, respectively shown in Figure 3a.

Spatially, the rainfall-erosivity distribution was not uniform in the study area due to variation in rainfall shown in (Figure 3b). It declined from the southwest portions of the sub-basin to the center and northern-west portions of the watershed. This highlights that the observed variance in erosivity within the area, all areas have considerably contributed to the overall loss of soil because water erosion is dependent at 80% on the erosivity values (Kidane et al., 2019; Meusburger et al., 2012). These values are low compared to those reported in Gumara watershed North-western in Dega Damot, Ethiopia, which range from 1,013.45 to 1,157.77 MJ mm/ha/hr/year (Belayneh et al., 2019) and higher than those reported in Dijo watershed, Rift valley Basin of Ethiopia, which range from 376 to 465 MJ mm/ha/year (Bekele & Gemi, 2021). Since *R*-factor is proportional to annual rainfall, the variation in *R*-factor is due to the variation in annual rainfall. This indicates that areas with high annual rainfall have higher erosivity factor.

*The Soil-Erodibility Factor (*K*).* This factor was determined by analyzing the soil map from the soil map developed by FAO (2015) in Arc GIS 10.7 (Figure 4a). *K*-factor values were determined to produce a raster layer of the *K*-factor map from the established soil map of this particular area (Figure 4b).

Out of the nine main soil types in the study area, four of them are dominant, covering 92.45%, of which 28.57% (Andosols), 26.47% (Luvisols), 26.7% (Fluvisols), and 10.71% (Vertisols) had moderate to the maximum erodibility factor values. Luvisols and fluvisols, covering above half (53.17%) of the watershed have the maximum *K* value (0.25 t/ha/hr/MJ/ha/mm). Soils with $K > 0.040$ t/ha/hr/MJ/ha/mm have high

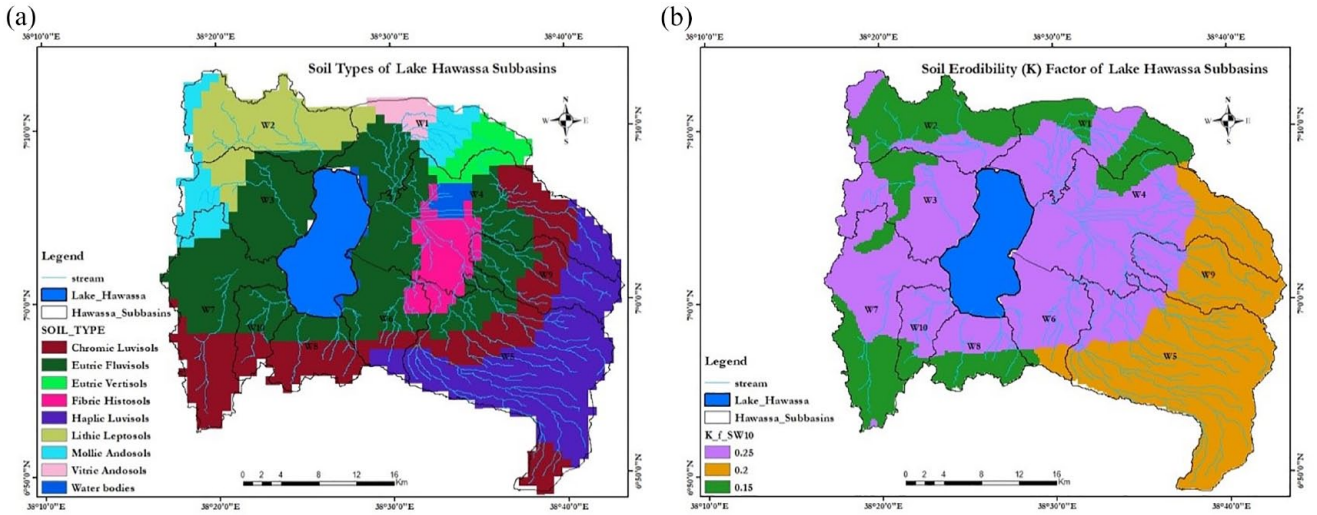

Figure 4. (a) Major soil unit type and (b) erodibility factor values.

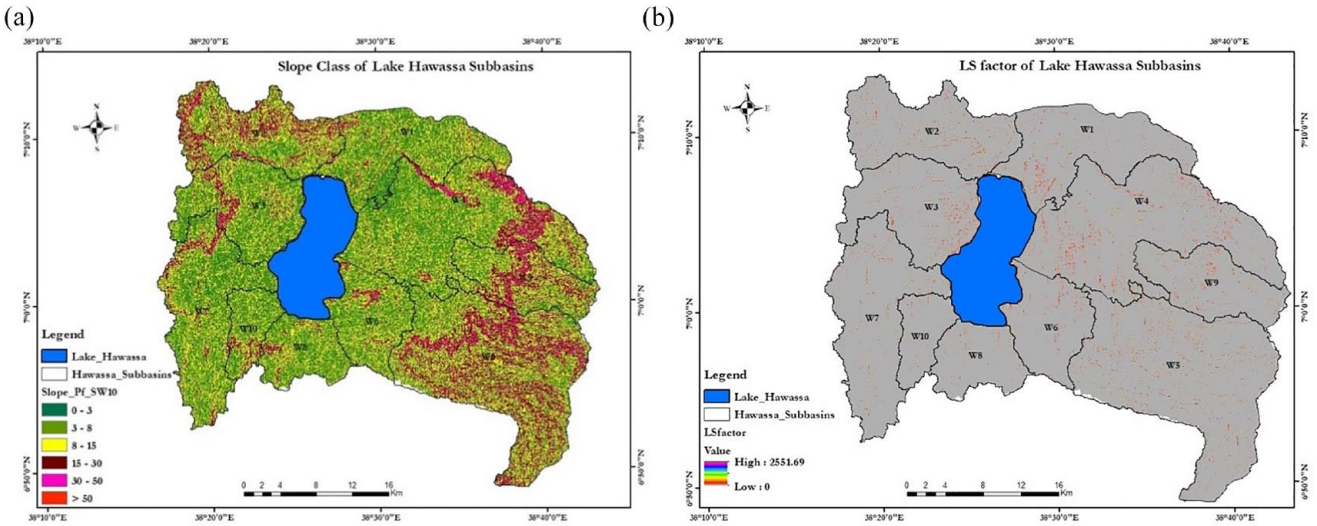

Figure 5. (a) Maps of slope and (b) steepness-length factor.

erodibility because of their low absorptivity and good structure (Dinka & Klik, 2019). However, almost all the soils in the watershed have a medium to high run-off future with high soil erodibility.

*Slope Length-Steepness Factors (*LS*).* The slope and corresponding slope steepness/*LS*/factor values are presented (Figures 4a and b). The landscape of the watershed is defined by a hilly and undulant landscape at higher elevations and a flat topography in its lowermost portion (Figure 5a). The slope was classified as 0–3, 3–8, 8–15, 15–30, 30–50, and >50% respectively, and it was covered 19.3, 28.5, 19.8, 17.7, 11.6, and 3.17% of the Lake subbasin respectively as shown in Table 7. The outcome indicated that the *LS* factor varied from 0 in the gentler slope at the lower part to 2,551.69 in the gentlest slope uphill part of the Lake subbasin (Figure. 5b). Thus, the upper portion of the sub-basin with the combined slope length-steepness (*LS*) component has a considerably high impact on soil loss. In contrast, in the lower and central parts of the sub-basin, the slope length-steepness element has a medium to low effect on soil erosion.

The results indicate that the northern-western, northern, and eastern higher portions have predominately high *LS*-factor, and those districts are distinguished by extremely steep gradients. These locations have slopes that are longer and steeper, which makes the runoff drive faster. Higher *LS* variables favor higher runoff, erosion, and sediment output, which facilitate silt deposition in the sunken portion of the catchment (Dinka, 2020; Phinzi & Ngetar, 2019).

*Land Covers (*C*) Factor.* Figure 6a, which showed the study area's current land-use/land-cover, provides an overview of the current conditions the study area. The *C*-factor map of the cover types generating the cover management-factor map for the sub-basin, and then its values were allocated for all cover

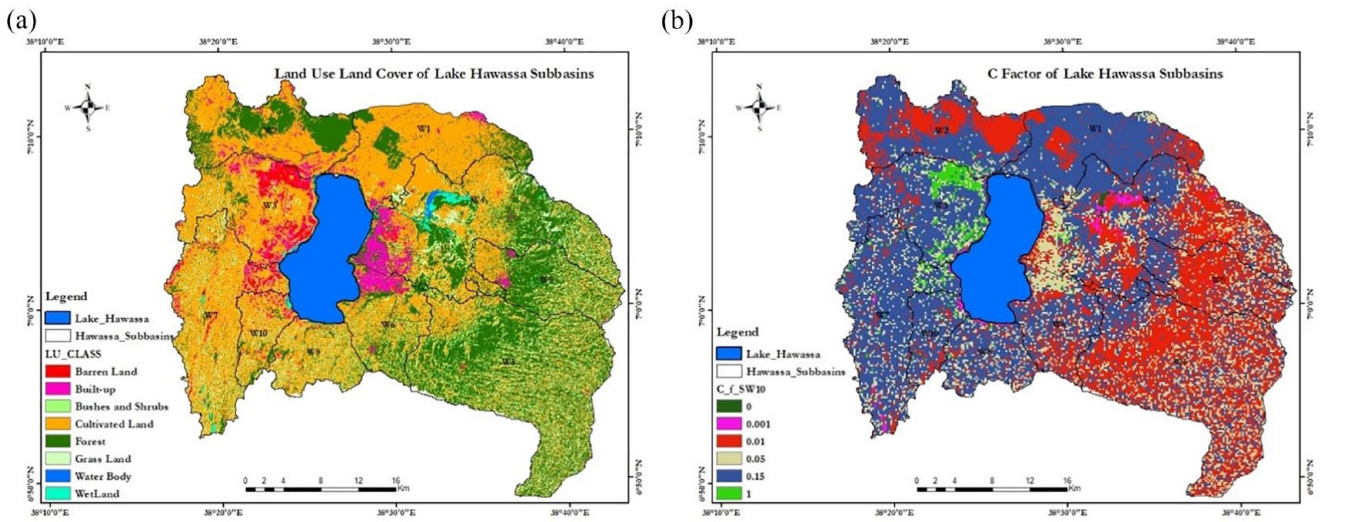

Figure 6. Map of LULC (a) and cover management (b).

Table 3. Cover Management (*C*) Factor Values.

LAND-USE COVER TYPES	*C*-FACTOR	AREA (HA)	%	SOURCES
Water body	0	10,579.69	6.75	Degife et al. (2019)
Wetland	0.001	5,702.11	4.02	Hurni (1985)
Forest	0.01	27,552.76	15.60	Hurni (1985)
Bushes and shrubs	0.05	7, 905.72	7.65	Wischmeier and Smith (1978)
Grass land	0.05	2,969.75	6.91	Hurni (1985)
Built-up	0.05	6,076.89	5.59	Degife et al. (2019) and Dinka (2020)
Cultivated land	0.25	70,054.15	48.48	Hurni (1985)
Barren land	1	4,550.54	5.02	Hurni (1985)

type in the sub-basin to come up with the cover factor map (Figure 6b). Nine LULC classes were classified and their corresponding *C*-values were determined based on a thorough evaluation of studies of a similar kind (Kidane et al., 2019; Molla & Sisheber, 2017) and as presented in Table 3.

The *C* values show that the surfaces that generate high runoff and make the soil particularly vulnerable to erosion are cultivated and barren lands, whereas water bodies and permanent wetlands receive the lowest values.

Soil erosion is significantly affected by the LULC conditions of the watershed, according to the present land cover analysis findings (Table 3). This conclusion is consistent with prior findings showing that vegetation significantly decreased soil loss and sediment yield (Ebabu et al., 2019; Kidane et al., 2019; Thomas et al., 2018).

*Land Use Management Practice Factor (*P*).* The assigned *P*-factor values presented, the agricultural lands located at various slopes were classified into six classes and were assigned with the practice factor varies from 0.1 to 0.33 as per the method of Wischmeier and Smith (1978). The sub-basin had a large distribution of cultivated land units, and Table 4 describes the value of the *P* factor in terms of cultivation method and slope (Bardgett & Shine, 1999).

Thus, the flatter gradients have minimum low *p* values, whereas steeper gradients have a maximum higher *p* value. The extent and spatial dissemination of the values of *p* are shown in Figure 7.

Soil Loss

The soil loss rate of the sub-catchment ranged from 0 (at the lower reach of Lake Hawassa) to 539.56 tonnes per pixel or 86.33 t/ha/year, where 1 pixel (250 × 250 m = 6.25 ha) with the average value in each pixel was 95.45 tonnes per pixel (16.36 t/ha/year). From the effective watershed area (120,383.17 ha) after excluding the water body and swamp from the analysis of (15,681.81 ha); the total annual base of soil loss was found to be 1.97 million t/year presented in Figure 8a.

Table 4. Land Cover Management Practice Factor (*P*).

LAND USE TYPE	CULTIVATED						OTHERS
Slope range	0–5	5–10	10–20	20–30	30–50	>50	—
P factor	0.1	0.12	0.14	0.19	0.25	0.33	1
Area (ha)	35,095.91	13,654.14	8,933.80	3,898.64	7,512.21	2,233.99	64,331.08
Area (%)	25.87	10.06	6.59	2.87	5.54	1.65	47.42

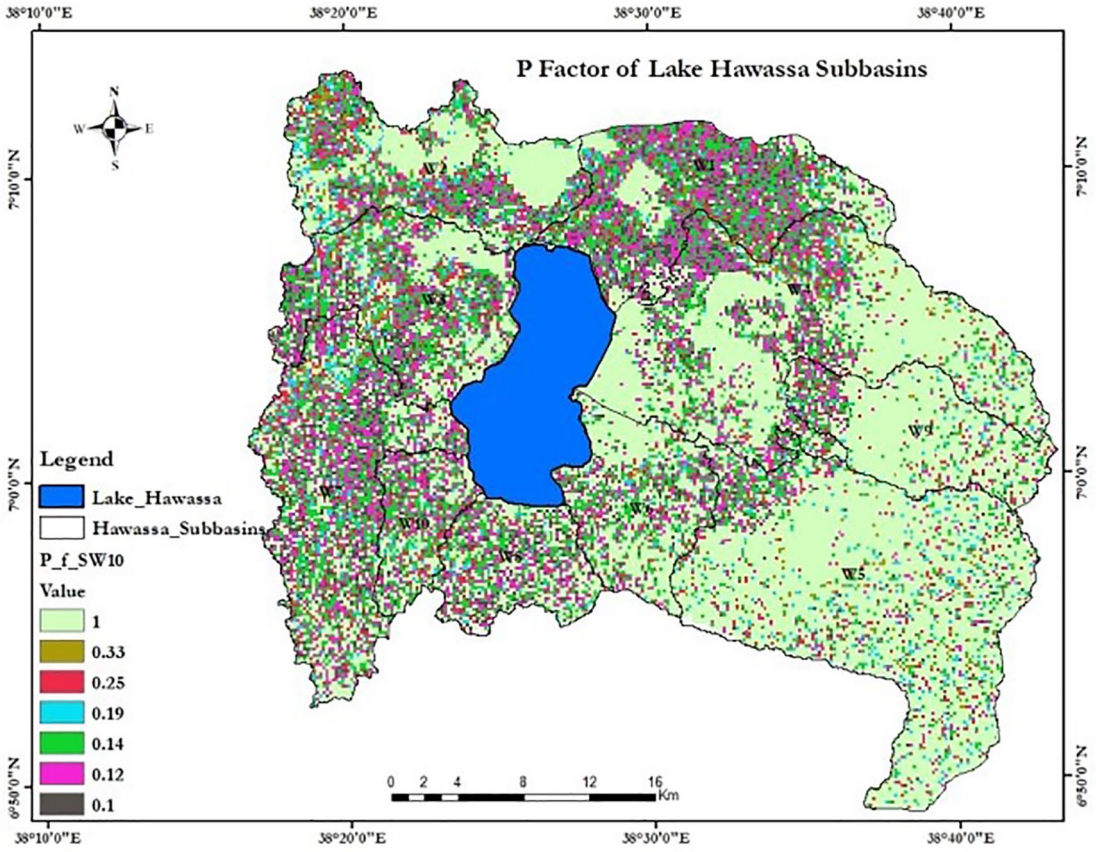

Figure 7. Map of land cover management practice (*P*) factor.

Figure 8a and b, shows that northern, eastern and western portion of the Lake sub-basin were noted with high soil loss rates. Field observation conducted to verify the results showed these portions of the area are dominated by cultivated land, barren land, degraded with steep slope, thus, no mooch that these areas are under high soil loss rate. Figure 8a was further classified to develop erosion severity class map (Figure 8b). Accordingly, the flatter slopes of the sub-basin fall under low soil loss severity class.

A comparison was made between the results and those of other studies conducted in various parts of Ethiopia with consideration of similar agro-ecologies. Thus, topography (slope length and gradient) and climate zone factors were identified as the main factors affecting soil erosion.

Severity Classes Soil Loss

Owing to various land uses and management techniques, different places have experienced varied soil losses, which may be compared according to the classification of erosion classes. This will help rank erosion hotspot regions and provide timely information for decision makers in planning the correct soil conservation actions according to their level of threat with the available resources (Tsegaye & Bharti, 2022; Wagari et al., 2024). The various severity soil loss classes, and the qualitative classification of soil loss rate severity classes was made based on the severity soil loss rate classifications of Ouyang and Bartholic (1997), as presented in Table 5, and the same classification was used by Haregeweyn et al. (2017), Yesuph and Dagnew (2019),

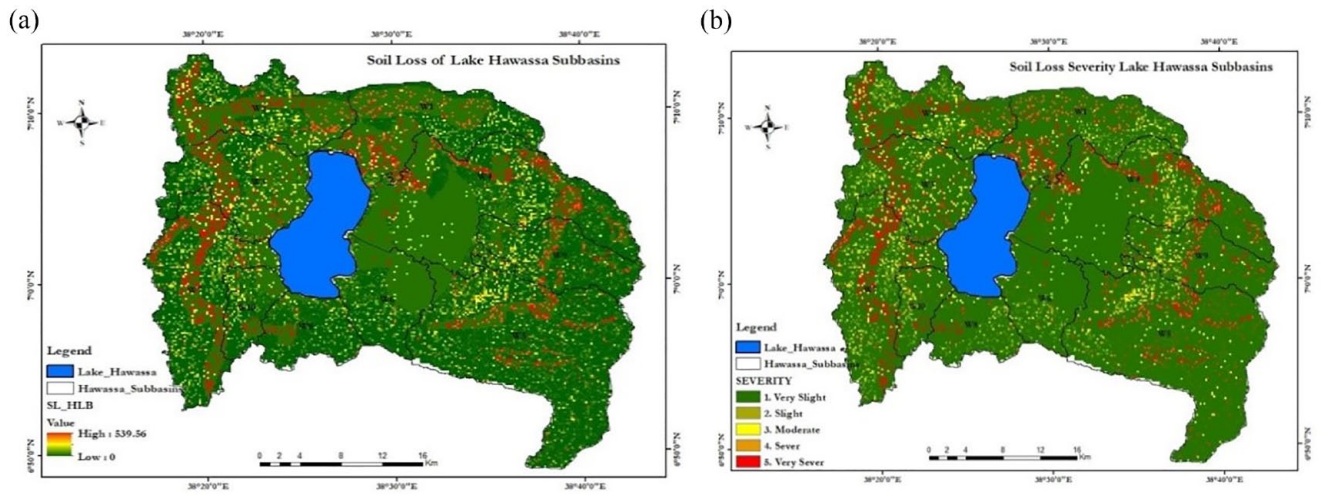

Figure 8. (a) Soil loss and (b) severity map of Lake Hawassa sub-basin.

Table 5. Sub-Catchment of Different Soil Loss Severity Class Area Coverage.

SMALL-CATCHMENTS	TOTAL EFFECTIVE AREA IN KM²	SOIL LOSS SEVERITY CLASS AND AREA COVERAGE IN PERCENTAGE									
		VERY-SLIGHT		SLIGHT		MODERATE		SEVER		VERY-SEVER	
		(0–5)		(5–10)		(10–25)		(25–45)		(>45)	
		KM²	%	KM²	%	KM²	%	KM²	%	KM²	%
1	118.07	48.7	41.25	33.9	28.71	11.60	9.82	10.16	8.6	13.11	11.1
2	102.03	33.98	33.3	20.1	19.7	13.47	13.2	14.45	14.2	20.06	19.6
3	109.94	38.8	39.5	26.5	24.1	15.76	13.3	12.106	10.2	17.81	19.58
4	209.43	87.75	41.9	55.92	26.7	30.37	14.5	15.91	7.6	19.48	9.3
5	160.94	59.06	36.7	27.84	17.3	19.79	12.3	24.3	15.1	29.93	18.6
6	84.67	42.93	50.7	22.18	26.2	14.82	17.5	2.03	2.4	2.71	3.2
7	231.38	90.7	39.2	43.037	18.6	30.774	13.3	25.915	11.2	40.954	17.7
8	59.50	19.75	33.2	13.03	21.9	5.83	9.8	8.03	13.5	12.85	21.6
9	89.66	29.41	32.8	15.42	17.2	12.104	13.5	14.17	15.8	18.56	20.7
10	38.21	16.01	41.9	8.52	22.3	3.13	8.2	4.7	12.3	5.85	15.3
T/Av	1,203.83	467.0	39.0	266.01	22.3	158.02	12.5	132.04	11.1	181.31	15.7

Note. 1, 2, 3. . .=sub small-catchments code (1 to 10); T/Av.=total average soil loss distribution of Lake Hawassa sub-basin.

and Degife et al. (2021) using the RUSLE model. The result of RUSLE model output of diverse degrees of soil loss severity indicated the area pattern of the different soil severities of the small catchments level; these are labelled in numbers from 1 to 10 of these ten catchments: sub-catchments 2, 3, 5, 7, 8, 9, and 10 were very susceptible to soil erosion.

In Table 5, the estimated annual soil loss area and percentage coverage as well as the total average value of the lake sub-basin are displayed along with the specific geographical variation of the soil loss for the separate small division sub-catchments.

The highest proportion (39%) of Lake Hawassa sub-basin is categorized under very slight (0–5 t/ha/year), 22.3% of the Lake sub-basin area the slight (5–10 t/ha/year), and 12.5% the moderate (10–25 t/ha/year) class of soil loss respectively. the Lake sub-basin, 11.1% had severe (25–45 t/ha/year) and 15.7% (>45 t/ha/year) the very severe soil loss rate class out of the total area of the sub-basin, with their erosion hotspot areas presented in Table 5 above. In addition, the qualitative classification of soil losses in the sub-basin was also computed to prioritize the erosion hazard regions (Figure 8b) at a small catchment level. Thus,

Table 6. Min., Maximum and Mean Soil Losses of Catchments in Lake-Hawassa Sub-Basin.

SMALL-CATCHMENTS	AREA (KM^2)	SOIL LOSS (T/HA/YEAR)			AREA-CONTRIBUTION SOIL LOSS IN (%)
		MIN.	MAX.	MEAN	
1	118.07	Near zero	87.2	21.29	9.81
2	102.03	>>	145	16.06	8.48
3	109.94	>>	154.2	24.92	9.13
4	209.43	>>	301.9	33.13	17.4
5	160.94	>>	137.4	14.17	13.37
6	84.67	>>	187.6	35.49	7.03
7	231.38	>>	217.0	46.24	19.22
8	59.50	>>	121.6	17.74	4.94
9	89.66	>>	88.8	11.23	7.45
10	38.21	>>	93.23	7.34	3.17
Overall mean annual sediment yield of LHSB				227.61	100

Note. Sub-catchment 5 and 9 is not added to the sediment yield in the whole catchment because it is not connected to the main study system of Lake Hawassa. as shown table 6, except for catchments 1, 8, 9, and 10; the average soil loss rates of all catchments were above the tolerable limit range of Ethiopia, which was above 12 t/ha/year (Hurni, 1985). This is mostly associated with land use/land cover and a higher steep gradient (Belete et al., 2021; Degife et al., 2019; Gebre et al., 2023).

Table 7. Annual Soil Loss Rate Under Different Slope Classes.

S. NO.	SLOPE RANGES	AREA (HA)	AREA (%)	SOIL LOSS RATE (T/YEAR)	SOIL LOSS CONTRIBUTION (%)	SOIL LOSS (T/HA/YEAR)
1	0–3	23,184.75	19.26	64,221.76	3.26	2.77
2	3–8	34,276.99	28.47	174,254.60	8.85	5.08
3	8–15	23,835.89	19.8	298,635.17	15.17	12.54
4	15–30	21,360.68	17.74	533,518.25	27.11	24.98
5	30–50	13,911.97	11.56	594,215.76	30.19	42.71
6	>50	3,812.79	3.17	279,559.94	14.20	73.32
Total		120,383.17	100.00	1,968,256.44	100.00	16.36

soil loss varied significantly from catchment to catchment, as shown in Table 6.

Soil Loss Rate Under Different Slope Classes

The slope map of the small catchments was classified based on the slope classes defined for Ethiopia by FAO (2006): flat, gentle slope, sloping, moderately steep, steep and very steep, with the slope ranges given in Table 7. The soil loss rate of the lake sub-basin varied significantly depending on the range of slope classes. The results in Table 7 show that the sub-basin with a slope of up to 15% of the area (67.43%) and the slope of >15% of the area (32.47%) contributed 27.29% and 71.5% of the soil loss respectively. The slope between 8% and 30% contributed 42.8% of the soil loss. There was a linear relationship, that is, as the slope increased, the soil loss per area (ha) increased.

The overall patterns of the results showed that soil loss and supply increased as the steepness of the slope of the watershed increased (Table 7).

Soil Loss Under Different LULC Classes

Land use/cover plays an important role in the assessment of erosion, while different land use/cover classes have different erosion rates.

The results showed that soil loss rates varied significantly from one LULC type to another. From the model results presented (Table 8), the maximum contributor to total soil loss is

Table 8. Soil Loss Rate Distribution in Different Land Use/Cover After Water Body and Marshland.

NO.	LAND-USE/ COVER TYPES	AREA (HA)	AREA (%)	SOIL LOSS (T/YEAR)	SOIL LOSS (%)	AVERAGE SOIL LOSS (T/HA/YEAR
1	Water body	10,579.69	7.8	—	—	—
2	Marshland	5,701.81	4.02	—	—	—
3	Forest	27,552.76	20.31	19,497.79	0.99	0.71
4	Urban area	6,076.52	5.59	57,593.04	3.15	9.48
5	Shrub land	7,905.72	7.65	54,248.92	2.96	6.86
6	Grassland	2,969.38	6.90	53,224.6	2.9	38.13
7	Cultivated land	71,328.69	52.31	1,559,121.00	84.96	21.86
8	Barren Land	4,550.20	5.02	91,384.04	4.98	20.08
	Total	136,664.77	100.00	1,969,536.54	100	16.36

Table 9. Minimum, Maximum and Average Sediment Delivery Ratio and Sediment Yield Individual Catchments.

INDIVIDUAL CATCHMENTS	AREA (KM^2)	SOIL LOSS (T/HA/YEAR)			AVERAGE SDR	SEDIMENT YIELD (T/HA/YEAR)	SEDIMENT YIELD (MMC)	AREA CONTRIBUTION SY (%)
		MIN	MAX	MEAN		MEAN		
1	118.07	Near zero	87.2	21.29	0.139	3.6	0.075	9.81
2	102.03	>>	145	16.06	0.146	3.12	0.052	8.48
3	109.94	>>	154.2	24.92	0.137	4.31	0.078	9.13
4	209.43	>>	301.9	33.13	0.350	7.39	0.304	17.4
5	160.94	>>	137.4	14.17	0.405	5.74	0.190	13.37
6	84.67	>>	187.6	35.49	0.164	6.25	0.087	7.03
7	231.38	>>	217.0	46.24	0.163	7.72	0.295	19.22
8	59.50	>>	121.6	17.74	0.417	7.41	0.073	4.94
9	89.66	>>	88.8	11.23	0.444	4.99	0.074	7.45
10	38.21	>>	93.23	7.34	0.122	0.895	0.006	3.17
	Overall SY of LHSB with average SDR 0.249						0.97	100.00

cultivated land (84.96%), and then the next is by barren land (4.64%). small contribution is the forest, which was less than 1%. The highest soil loss is predicted for cultivated land with a mean annual soil loss rate of 21.86 t/ha/year, followed by barren land and grassland with mean annual soil loss rates of 20.08 and 17.92 t/ha/year respectively.

Estimation of Sediment Delivery Ratio (SDR)

The spatial pattern of the SDR map was generated, and its value was quantified for channels in the study sub-basin, as shown in Table 9 and Figure 9a and b, for the purpose of sediment yield determination. The SDR varies significantly from catchment to catchment, and its minimum mean value is rich in lower catchments (catchment 10) with a value of 0.122. The maximum mean value (0.444) was observed at the steepest upper catchment (catchment 9).

This suggests that the detached constituents were transported to the river network system and added to sediment production of lowest of 12.2% to highest of 44.4%. Thus, the SDR variation can be related to the channel slope, that is, at the highest, intermediate, and gentle channel slopes, the SDR values are the highest, moderate, and low, respectively. The study Lake Sub-basin average sediment delivery capability is approximately

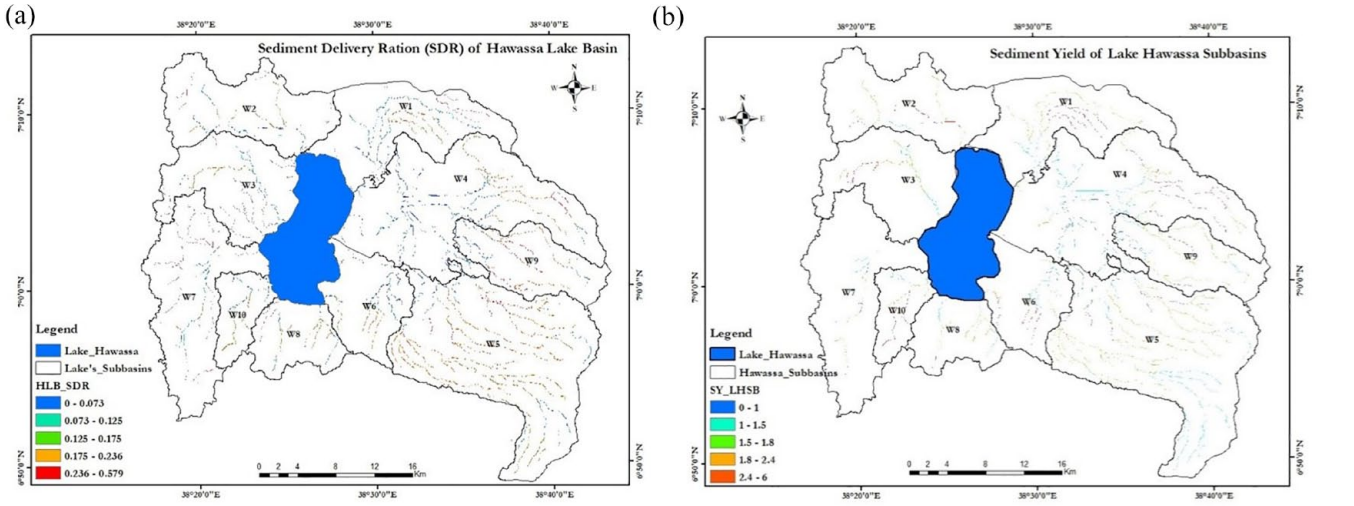

Figure 9. (a) Sediment delivery ratio and (b) sediment yield map.

0.249, that is, 24.9% of the eroded soil constituents may be transported to the lake outlet, while 75.1% of the eroded materials are retained and deposited within the sub-basin.

Sediment Yield (SY) Estimation

The sediment yield at the outlet of the lake was calculated using the channel network gradient by the Sediment Delivery Ratio model developed by Williams and Berndt (1977) cited in Gelagay and Minale (2016). Thus, the sediment delivery ratio (SDR) and average annual soil loss raster layer was multiplied cell-by-cell to create a geographically distributed map of sediment yield. By combining soil loss and SDR raster layers, that is, the watershed's average soil loss (16.36 t/ha/year) and its total SDR (24.9%) were multiplied to obtain the sediment output.

These two variables resulted in an average sediment yield of 4.07 t/ha/year at the sub-basin outlet point. Additionally, the average size of the sediment yield for each small catchment was estimated; hence, the sediment yield for each small catchment is shown in Table 9 in terms of the amount of silt supplied at the outlet point (t/ha/year). The sediment yield at the outflow grid cell is represented in Figure 8b and was calculated by multiplying the total soil loss from the entire watershed by the SDR value of the grid cell. According to the sediment field map and Table 9, the sub-basin Sediment Yield (SY) varies in a manner that is spatially consistent with the soil loss and sediment delivery ratio maps.

Prediction the Lake Depth and Its Volume Loss Rate

It was discussed in result Section pesernted in Table 9, the lake receives 0.97 million m^3 of sediment per year from rill and sheet erosion, which is transported and deposited in the lake by eight drainage systems from the entire 10 catchments. Therefore, the distribution of sediment transported to and deposited in the lake was calculated by taking into account the lake's constant volume loss per year (0.97 million m^3/year) and constant surface area (95.57 million m^2) as determined by Gebre et al. (2023). Thus, the thickness of sediment received by the lake per year from sheet and rill erosion is 1.01 cm, which was obtained by dividing the volume of sediment entering the lake by the surface area of the lake.

Assessment of Land Use Policy Implementation

Land use policy implementation was assessed based on the current land use/land cover condition and slope class of rural land use policy criteria (Alemu, 2011) with the support of field observations. This land-use policy is mainly concerned with land management practices developed on the basis of the steepness/slopes/of the land. The slope classification was based on Ethiopia's Rural Land Administration and Land-Use Proclamation No. 456/2005 (Alemu, 2011).

From field observations and slope class recommendations, land use policy implementation was weak and not applied to grassroots. Thus, both the study findings and field observations indicated that, about 24.2% area or 31,675 ha of the land was cultivated on slopes greater than 15% (steep slope) in the Lake sub-basin without application of any of the conservation practices mentioned in land-use policy of Ethiopia. Out Of these cultivated lands, 9.55% (13,773.84 ha), 2.87% (3,898.64 ha), 5.54% (7,512.21 ha), and 1.65% (2,233.99 ha) were found in steepness greater than and in between 15, 20–30, 30–50 and >50%, respectively, in which one of the major sources soil erosion prone areas next to barren and grass lands (see on Table 4). Thus, it can be said that weak implementation of the policy and lack of follow-up are among the major problems that the lake sub-basin suffers from soil erosion.

Discussion

The soil loss rate is range from 0 (at the lower reach of Lake Hawassa) to 86.33 t/ha/year with the average value 13.36 t/ha/year. Thus, the total annual base of soil loss was found

to be 1.97 million t/year from the effective watershed area (120,383.17 ha). The finding shows that northern, eastern and western portion of the Lake sub-basin were noted with high soil loss rates. Field observation conducted to verify the results showed these portions of the area are dominated by cultivated land, barren land, degraded with steep slope and populated urban areas. A comparison was made between the results and those of other studies conducted in various parts of Ethiopia with consideration of similar agro-ecologies. The soil loss was found to be slightly larger than the acceptable soil losses determined for various agro-climatic zones of Ethiopia (6 t/ha/year estimated for dry Weynadega, 8 t/ha/year for Moist Dega and 12 t/ha/year for Moist Weynadega (Hurni, 1985). The agro-ecological and climatic settings of the Lake Watershed fall under these three categories. Therefore, the average soil loss of the sub-basin (16.36 t/ha/year) which is higher than the allowable soil loss value 12 t/ha/year (Hurni, 1985). These variations can be attributed to variations in climatic factor, topographic (slope length and gradient) and land use/land cover conditions with time (Y. Abebe et al., 2018; Belete et al., 2021; Degife et al., 2019) were identified as the main factors affecting soil erosion.

The soil loss of the study was also found to be larger than other studies by 2.2 t/ha/year by 9.1 t/ha/year that of Dijo and Zingin watershed respectively (Ayalew, 2015; Bekele & Gemi, 2021). On the other hand, the soil loss in the Lake sub-basin was found to be less than 23.7, 32.8, 41.5, 42.7, 47, 49, and 93 t/ha/years in the Gelda, Gilgel Abay, Megech, Gumara, and Koga watersheds (Balabathina et al., 2019; Belayneh et al., 2019; Gashaw et al., 2018, 2020; Gelagay & Minale, 2016; Moges & Holden, 2007; Zerihun et al., 2018) respectively, in different parts of Ethiopia.

Soil loss under different slope class and LULC was estimated based on the slope classes defined for Ethiopia by FAO (2006) and in different LULC attributes. The soil loss rate was varied significantly depending on the range of slope classes thus, the slope of up to 15% of the area (67.43%) and the slope of >15% of the area (32.47%) contributed 27.29% and 71.5% of the soil loss respectively. The patterns of the results showed that soil loss and supply increased as the steepness of the slope of the watershed increased. This is realistic, and the area with steeper slopes is more vulnerable than the areas with lower steep slopes (Belete et al., 2021). The soil loss rates under different land use/cover classes have given different erosion rates and it was varied significantly from one LULC type to another. The highest soil loss is predicted for cultivated land with a mean annual soil loss rate of 21.86 t/ha/year, followed by barren land and grassland with mean annual soil loss rates of 20.08 and 17.92 t/ha/year respectively. Thus, arable land has the highest soil loss rate compared to other land uses, as most of the arable land is located on the steepest slope of the Lake basin. This can be attributed to the fact that even steep slopes have been cultivated. In the study area, 24.65% or 31,675.84 ha of the land with steep slopes (>15%) is cultivated in the sub-basin and a high erosion rate is expected, which can generate a higher sedimentation rate into the lake in all directions. This is in agreement with the results of studies carried out in the same area, where moderately and intensively cultivated areas in the steep part of the catchment are possible sources of sediment (Belete et al., 2021; Degife et al., 2019). The forest area had the lowest soil loss rate, followed by agroforestry, which is in agreement with Hurni (1985) and seems to be consistent with natural processes.

The spatial pattern of the SDR map was generated, and its value was quantified for channels in the study sub-basin. The SDR varies significantly from catchment to catchment with minimum and maximum mean value of 0.122 and 0.444 values was at rich in lower and at the steepest upper catchment respectively. This suggests that the detached constituents were transported to the river network system and added to sediment production of lowest of 12.2% to highest of 44.4%. The average sediment delivery capability is approximately 0.249, that is, 24.9% of the eroded soil constituents may be transported to the lake outlet, while 75.1% of the eroded materials are retained and deposited within the sub-basin. The SDR variation can be related to the channel slope, that is, at the highest, intermediate, and gentle channel slopes, the SDR values are the highest, moderate, and low, respectively. Because it accurately shows the critical characteristics of sediment delivery that erosion takes place in a steeper location will have more opportunities to be conveyed in the river networks than deposited in the downslope, the SDR map was thought to be realistic. Thus, this study indicates that steeper areas with close proximity to the tributary network and narrower upper watersheds of the sub-basin have higher SDR values than the middle and lower catchments of the Lake sub-basin, which are flatter and larger areas. According to Mutua and Klik (2006) and Gelagay and Minale (2016) catchments with steep gradients, small drainage areas, and districts close to watercourses transport sediment at an advanced rate than those with wide, flat valleys, large drainage areas, and fields far from streams. Therefore, the estimation of the sediment delivery ratio in a spatially dispersed (cell-based) form enables the identification of important sediment sources and delivery sites as well as the site-specific application of appropriate management techniques within the sub-basin.

The Lake average sediment yield of 4.07 t/ha/year at the sub-basin outlet point resulted from the combing of average soil loss and SDR of the study Lake Basin. Additionally, the average size of the sediment yield for each small catchment was estimated. According to the sediment field map, the sub-basin Sediment Yield (SY) varies in a manner that is spatially consistent with the soil loss and sediment delivery ratio maps. The watershed's steeper, narrower, and more degraded catchment area is where the average greatest annual sediment source areas are located, while the catchments with flatter slopes and wider drainage sections had the lowest values. The primary soil type that is prone to erosion and steep slope (high *LS* factor value) could be the affect; as a result, very high or low computed soil loss is characterized by high and low channel slopes, short and long distances from the field to

the stream, and abundant order streams, resulting in very high or low sediment delivery capacities (Gelagay & Minale, 2016; Mutua & Klik, 2006).

The total amount of sediment generated was 3.805 million m^3, which is the result of this study (sediment yield of 0.97 million m^3 from sheet and gully erosion generated by the RUSLE model and 2.835 million m^3 from gully erosion as investigated by Gebre et al. (2023). The thickness of silt deposited 3.98 cm/year, obtained by assuming the constant rate volume (3.805 million m^3) sediment added to the lake bed and by taking the lake surface area of 95.57 million m^2 (Gebre et al., 2023) the sediment thickness from the gully contribution 2.97 cm/year (Gebre et al., 2023) whereas 1.01 cm/year from sheet and rill erosions. Dividing the sediment yield from the study outcome (3.805 million m^3) by taking the Lake volume of 1,174.61 million m^3 (Y. Abebe et al., 2018; the Lake annual reduction in storage capacity could be estimated at 0.32%/year with the Lake life span of 303 years. This is supported by other studies (Y. Abebe et al., 2018; Belete et al., 2021; Menberu et al., 2021) shown that siltation from the sub-basin catchment, caused by sheets, gullies and gullies, and from other sources like solid waste from the town of Hawassa, at a rate of 0.33% (4.76 million m^3) and 4% (46.67 million m^3) reduction in the volume of the lake over the period 1999 to 2011 (Belete et al., 2021; Gebre et al., 2023; Menberu et al., 2021). This was less than the estimated global mean of 1% per year in storage loss (Church, 2001). Similarly, the estimated annual volume loss of Lake Hawassa is lower than that of Lake Tana (Lemma et al., 2018) and higher than that of Lake Ziway in the Ethiopian Rift Valley (Aga et al., 2019).

To prevent soil loss from steepest cultivated lands, converting farmland into forest or perennial crop land is a recommended option called land-use de-strengthening, which refers to the modification of erosion-susceptible land to non-erosion-susceptible land use. Because it is not favored by local farmers, it is rather difficult to convert farmed land or cropland into woodland in much of the study region. It is advised as a remedy to convert agricultural land with slopes of more than 15% to agroforestry land-use suggested by Mtibaa et al. (2018). This practice may be more advantageous for local farmers and promote the government's agricultural policy, which aims to expand the output of cash crops and fruit. Slopes greater than 60% should be used to define the boundaries of the forestland. Reducing soil loss and sediment yield from the sub-basin should be made possible by using additional workable crop management and erosion control techniques (such as reduced tillage and channel control) and focusing on regions with significant water erosion potentials.

Limitation of the Study

The study was investigated by using RUSLE and SDR model, the models result uncertain due to lack of observed data for validation of the predicted results. To overcome this problem, field based observation was made by researchers to check the actual condition of each sub-catchment's that contributed the soil loss for the sub-basin. The field observation confirmed that, the predicted high soil loss was found in the sub-catchment with dominated of cultivated land steepest area, barren and grass lands whereas, the lowest soil loss predicted was found in the forest cover area of the sub-catchments. In addition, this comparison was made by reviewing other studies carried out in the same agro-ecological and climatic setting of the country among the validation approach which was mention in "Validation and Consistency of the Model Outputs" section. The soil loss and sediment generated by the RUSLE and SDR model in the lake basin is only from sheet and rill portion of water erosion, this can't include the road and drainage network system carried solid waste from Hawassa town to the lake body additional sources of lake sedimentation mentioned by Belete (2020); needs to be further investigation to explore additional capacity the sediment generated from this sources to fill the exact figure of Lake sedimentation rate.

Conclusion

For effective management of water and land resources, sound knowledge and availability of information on the spatial distribution of soil loss and sediment yield appear to be more important than gross annual soil loss. The annual soil loss rate of the catchment ranged from 0 to 86.33 t/ha/year with a total annual soil loss of 16.36 t/ha/year with a mean sediment yield of 4.07 t/ha/year. Significant soil erosion was observed on sloppy cultivated, barren and grass land with mean annual soil loss of 21.86, 20.08, and 17.92 t/ha/year, respectively; while 2.77 and 73.32 t/ha/year were found on the lowest and steepest slopes, respectively. A spatially distributed Sediment Delivery Ratio (SDR) map that was generated for channels at a small catchment level showed on average 24.9% of the eroded soil material was delivered to the Lake. The annual sedimentation thickness from sheet and rill erosion of 1.01 cm/year was observed: taking the ratio of the sediment yield of 0.97 million m^3/year with the 2023 surface area of 95.57 million m^2. The land use of the study area indicated that the highest soil loss from the steepest area was cultivated without any conservation measures. Lack of policy enforcement at the grassroots level, as well as inappropriate land management practices deemed to be the main determinants of soil erosion in Lake Hawassa Sub-basin. The highest soil loss was associated with steeply sloping areas and cultivated barren and grassland dominated sub-basin. Therefore, in the steepest cultivated areas, the spatial variation of soil loss severity in the RUSLE and SDR models plays a crucial role in alerting land resource managers and all stakeholders to mitigate the consequences by implementing both structural and non-structural mitigation measures, requiring intensive efforts to reduce soil erosion and its associated problems.

Acknowledgements

We thank the United States Geological Survey (USGS) for providing Landsat Image support for this study at https://earthexplorer.usgs.gov/.

Author Contributions

Agegnehu Mitiku Gebre: Conceptualization (equal), data curation (equal), formal analysis (equal), investigation (lead), methodology (equal), software (equal), validation (equal), writing—original draft (equal). Mulugeta Dadi Belete: Data curation (equal); supervision (equal); writing—review and editing (equal). Moltot Zewude Belayneh: Supervision (equal); writing—review and editing (equal).

Funding

The author(s) received no financial support for the research, authorship, and/or publication of this article.

Declaration of Conflicting Interests

The author(s) declared no potential conflicts of interest with respect to the research, authorship, and/or publication of this article.

ORCID iDs

Agegnehu Mitiku Gebre https://orcid.org/0009-0001-9206-8154

Mulugeta Dadi Belete https://orcid.org/0000-0001-7781-7252

Data Availability Statement

The first Author can provide the data used in this study upon request.

REFERENCES

Abebe, T. G., & Woldemariam, A. (2024). Erosion spatial distribution mapping and sediment yield estimation using RUSLE and arc GIS of Ayigebire watershed, North Shewa zone of Amhara region, Ethiopia. *Water-Energy Nexus*. Advanced online publication. https://doi.org/10.1016/j.wen.2023.12.002

Abebe, Y., Bitew, M., Ayenew, T., Alo, C., Cherinet, A., & Dadi, M. (2018). Morphometric change detection of Lake Hawassa in the Ethiopian Rift Valley. *Water (Switzerland)*, 10(5), 1–15. https://doi.org/10.3390/w10050625

Aga, A. O., Chane, B., & Melesse, A. M. (2018). Soil erosion modelling and risk assessment in data Scarce Rift Valley Lake Regions, Ethiopia. *Water (Switzerland)*, 10(11). https://doi.org/10.3390/w10111684

Aga, A. O., Melesse, A. M., & Chane, B. (2019). Estimating the sediment flux and budget for a data limited Rift Valley Lake in Ethiopia. *Hydrology*, 6(1). https://doi.org/10.3390/hydrology6010001

Alemu, G. (2011). *Rural land policy, rural transformation and recent trends in large-scale rural acquisitions in Ethiopia* (pp. 1–28). European Report on Development, Overseas Development Institute (ODI). http://erd-report.eu/erd/report_2011/documents/dev-11-001-11researchpapers_alemu.pdf

Angima, S. D., Stott, D. E., O'Neill, M. K., Ong, C. K., & Weesies, G. A. (2003). Soil erosion prediction using RUSLE for central Kenyan highland conditions. *Agriculture, Ecosystems & Environment*, 97(1–3), 295–308. https://doi.org/10.1016/S0167-8809(03)00011-2

Arnold, J. G., Gassman, P. W., Reyes, M. R., & Green, C. H. (2007). The soil and water assessment tool: Historical development, applications, and future research directions. *Transactions of the ASABE*, 50(4), 1211–1250.

Asare, A., & Boye, C. B. (2021). Determination of soil erosion and sediment yield in the Bonsa River basin using GIS and revised universal soil loss equation (RUSLE). *Ghana Mining Journal*, 21(2), 1–11. https://doi.org/10.4314/gm.v21i2.1

Awulachew, S. B., Smakhtin, V., Molden, D., & Peden, D. (2017). *Nile River basin: Water agriculture, governance and livelihoods*. IWMI Books, International Water Management Institute.

Ayalew, G. (2015). A geographic information system based soil loss and sediment estimation in Zingin watershed for conservation planning, highlands of Ethiopia. *International Journal of Science, Technology and Society*, 3(1), 28. https://doi.org/10.11648/j.ijsts.20150301.14

Ayenew, B., Taddesse, A. M., Kibret, K., & Melese, A. (2018). Chemical forms of phosphorous and physicochemical properties of acid soils of Cheha and Dinsho districts, southern highlands of Ethiopia. *Environmental Systems Research*, 7(1), 1–15. https://doi.org/10.1186/s40068-018-0118-9

Balabathina, V., Raju, R. P., & Mulualem, W. (2019). Integrated remote sensing and GIS-based universal soil loss equation for soil erosion estimation in the Megech river catchment, Tana Lake sub-basin, Northwestern Ethiopia. *American Journal of Geographic Information System*, 4, 141–157. https://doi.org/10.5923/j.ajgis.20190804.01

Bardgett, R. D., & Shine, A. (1999). Linkages between plant litter diversity, soil microbial biomass and ecosystem function in temperate grasslands. *Soil Biology and Biochemistry*, 31(2), 317–321. https://doi.org/10.1016/S0038-0717(98)00121-7

Bekele, B., & Gemi, Y. (2021). Soil erosion risk and sediment yield assessment with universal soil loss equation and GIS: In Dijo watershed, Rift Valley basin of Ethiopia. *Modeling Earth Systems and Environment*, 7(1), 273–291. https://doi.org/10.1007/s40808-020-01017-z

Belay, H. T., Malede, D. A., & Geleta, F. B. (2020). Erosion risk potential assessment using GIS and RS for soil and water resource conservation plan: The case of Yisir watershed, northwestern Ethiopia. *Agriculture, Forestry and Fisheries*, 9(1), 1. https://doi.org/10.11648/j.aff.20200901.11

Belayneh, M., Yirgu, T., & Tsegaye, D. (2019). Effects of soil and water conservation practices on soil physicochemical properties in Gumara watershed, Upper Blue Nile basin, Ethiopia. *Ecological Processes*, 8(1), 1–14. https://doi.org/10.1186/s13717-019-0188-2

Belete, M. D. (2020). *Foundation for source-to-sea management: Characterization of sediment flows in Lake*. Stockholm International Water Institute (SIWI), Funded by Federal Ministry for Economic Cooperation and Development.

Belete, M. D., Hebart-Coleman, D., Mathews, R. E., & Zazu, C. (2021). Building foundations for source-to-sea management: the case of sediment management in the Lake Hawassa sub-basin of the Ethiopian Rift Valley. *Water International*, 46(2), 138–156. https://doi.org/10.1080/02508060.2021.1889868

Biondi, D., Freni, G., Iacobellis, V., Mascaro, G., & Montanari, A. (2012). Validation of hydrological models: Conceptual basis, methodological approaches and a proposal for a code of practice. *Physics and Chemistry of the Earth*, 42–44, 70–76. https://doi.org/10.1016/j.pce.2011.07.037

Camacho-Zorogast, C., Minga, J. C., Gómez-Lora, J. W, Gallo-Ramos, V. H., & Díaz, V. G. (2023). Evaluation of soil loss and sediment yield based on GIS and remote sensing techniques in a complex Amazon Mountain basin of Peru: Case study Mayo River basin, San Martin Region. *Sustainability*, 15(11), 9059.

Church, J. A. (2001). Sea level rise: History and consequences. *Eos, Transactions, American Geophysical Union*, 82(34), 376–376. https://doi.org/10.1029/01eo00232

Degife, A., Worku, H., & Gizaw, S. (2021). Environmental implications of soil erosion and sediment yield in Lake Hawassa watershed, south-central Ethiopia. *Environmental Systems Research*, 10(1). https://doi.org/10.1186/s40068-021-00232-6

Degife, A., Worku, H., Gizaw, S., & Legesse, A. (2019). Land use land cover dynamics, its drivers and environmental implications in Lake Hawassa watershed of Ethiopia. *Remote Sensing Applications: Society and Environment*, 14, 178–190. https://doi.org/10.1016/j.rsase.2019.03.005

den Biggelaar, C., Lal, R., Wiebe, K., & Breneman, V. (2003). The global impact of soil erosion on productivity. I: Absolute and relative erosion-induced yield losses. *Advances in Agronomy*, 81(3), 1–48. https://doi.org/10.1016/S0065-2113(03)81001-5

Dinka, M. O. (2020). Quantification of soil erosion and sediment yield for ungauged catchment using the RUSLE model: Case study for Lake Basaka catchment in Ethiopia. *Lake and Reservoir Research Management*, 25(2), 183–195. https://doi.org/10.1111/lre.12312

Dinka, M. O., & Klik, A. (2019). Effect of land use–land cover change on the regimes of surface runoff—The case of Lake Basaka catchment (Ethiopia). *Environmental Monitoring and Assessment*, 191(5), 278. https://doi.org/10.1007/s10661-019-7439-7

Ebabu, K., Tsunekawa, A., Haregeweyn, N., Adgo, E., Meshesha, D. T., Aklog, D., Masunaga, T., Tsubo, M., Sultan, D., Fenta, A. A., & Yibeltal, M. (2019). Effects of land use and sustainable land management practices on runoff and soil loss in the Upper Blue Nile basin, Ethiopia. *Science of the Total Environment*, 648, 1462–1475. https://doi.org/10.1016/j.scitotenv.2018.08.273

Endalew, T., & Biru, D. (2023). Soil erosion risk and sediment yield assessment with revised universal soil loss equation and GIS: The case of Nesha watershed,

Southwestern Ethiopia results in geophysical sciences soil erosion risk and sediment yield assessment with revised universal. *Results in Geophysical Sciences*, 12, 100049. https://doi.org/10.1016/j.ringps.2022.100049

Erol, A., Koşkan, Ö., & Başaran, M. A. (2015). Socioeconomic modifications of the universal soil loss equation. *Solid Earth*, 6(3), 1025–1035. https://doi.org/10.5194/se-6-1025-2015

FAO. (2006). Assessing soil loss by water erosion in Jamni River basin, Bundelkhand region, India, adopting universal soil loss equation using GIS. *Current Science*, 90(10), 1431–1435.

FAO. (2015). *Status of the world's soil resources*. http://www.fao.org/3/a-i5199e.pdf

Gashaw, T., Tulu, T., & Argaw, M. (2018). Erosion risk assessment for prioritization of conservation measures in Geleda watershed, Blue Nile basin, Ethiopia. *Environmental Systems Research*, 6(1), 1–14. https://doi.org/10.1186/s40068-016-0078-x

Gashaw, T., Worqlul, A. W., Dile, Y. T., Addisu, S., Bantider, A., & Zeleke, G. (2020). Evaluating potential impacts of land management practices on soil erosion in the Gilgel Abay watershed, Upper Blue Nile basin. *Heliyon*, 6(8), e04777. https://doi.org/10.1016/j.heliyon.2020.e04777

Gebre, A. M., Belete, M. D., & Belayneh, M. Z. (2023). Object-based image analysis (OBIA)-based gully erosion dynamics, sediment loading rate and sediment yield study in Lake Hawassa sub-basin, Ethiopia. *Natural Resource Modeling*, 36(3), e12368. https://doi.org/10.1111/nrm.12368

Gebrehiwot, S. G., Bewket, W., Gärdenäs, A. I., & Bishop, K. (2014). Forest cover change over four decades in the Blue Nile Basin, Ethiopia: Comparison of three watersheds. *Regional Environmental Change*, 14(1), 253–266. https://doi.org/10.1007/s10113-013-0483-x

Gelagay, H. S., & Minale, A. S. (2016). Soil loss estimation using GIS and Remote sensing techniques: A case of Koga watershed, Northwestern Ethiopia. *International Soil and Water Conservation Research*, 4(2), 126–136. https://doi.org/10.1016/j.iswcr.2016.01.002

Haregeweyn, N., Tsunekawa, A., Nyssen, J., Poesen, J., Tsubo, M., Tsegaye Meshesha, D., Schütt, B., Adgo, E., & Tegegne, F. (2015). Soil erosion and conservation in Ethiopia: A review. *Progress in Physical Geography*, 39(6), 750–774. https://doi.org/10.1177/0309133315598725

Haregeweyn, N., Tsunekawa, A., Poesen, J., Tsubo, M., Nyssen, J., Vanmaercke, M., Zenebe, A., Meshesha, D. T., & Adgo, E. (2015). Sediment Yield Variability at Various Spatial Scales and Its Hydrological and Geomorphological Impacts on Dam-catchments in the Ethiopian Highlands. *Landscapes and Landforms of Ethiopia*, 227–238. https://doi.org/10.1007/978-94-017-8026-1_13

Haregeweyn, N., Tsunekawa, A., Poesen, J., Tsubo, M., Meshesha, D. T., Fenta, A. A., Nyssen, J., & Adgo, E. (2017). Comprehensive assessment of soil erosion risk for better land use planning in river basins: Case study of the Upper Blue Nile River. *Science of the Total Environment*, 574, 95–108. https://doi.org/10.1016/j.scitotenv.2016.09.019

Hategekimana, Y., Allam, M., Meng, Q., Nie, Y., & Mohamed, E. (2020). Quantification of soil losses along the coastal protected areas in Kenya. *Land*, 9(5), 1–17. https://doi.org/10.3390/LAND9050137

Hui, L., Xiaoling, C., Lim, K. J., Xiaobin, C., & Sagong, M. (2010). Assessment of soil erosion and sediment yield in Liao watershed, Jiangxi Province, China, Using USLE, GIS, and RS. *Journal of Earth Science*, 21(6), 941–953. https://doi.org/10.1007/s12583-010-0147-4

Hurni, H. (1985). *Erosion-productivity-conservation systems in Ethiopia* [Conference session]. Proceedings of 4th International Conference on Soil Conservation, Maracay, Venezuela, November 3–9, 1985 (pp. 654–674).

Hurni, H. (2016). *Erosion-productivity-conservation systems in Ethiopia* [Conference session]. Conservation Systems in Ethiopia IV International Conference.

Karaburun, A. (2010). Estimation of C factor for soil erosion modeling using NDVI in Buyukcekmece watershed. *Ozean Journal of Applied Science*, 3(1), 77–85. http://ozelacademy.com/OJAS_v3n1_8.pdf

Kassay, A. B., Tuhar, A. W., & Ulsido, M. D. (2023). Integrated modelling techniques to implication of demographic change and urban expansion dynamics on water demand management of developing city in Lake Hawassa watershed, Ethiopia. *Environmental Research Communications*, 5(5), 512. https://doi.org/10.1088/2515-7620/acd512

Kidane, M., Bezie, A., Kesete, N., & Tolessa, T. (2019). The impact of land use and land cover (LULC) dynamics on soil erosion and sediment yield in Ethiopia. *Heliyon*, 5(12), e02981. https://doi.org/10.1016/j.heliyon.2019.e02981

Kulimushi, L. C., Choudhari, P., Mubalama, L. K., & Banswe, G. T. (2021). GIS and remote sensing-based assessment of soil erosion risk using RUSLE model in South-Kivu province, eastern, Democratic Republic of Congo. *Geomatics, Natural Hazards and Risk*, 12(1), 961–987. https://doi.org/10.1080/19475705.2021.1906759

Kumar, N., & Singh, S. K. (2021). *Soil erosion assessment using earth observation data in a trans-boundary river basin*. Vol 107. Springer. https://doi.org/10.1007/s11069-021-04571-6

Lemma, H., Admasu, T., Dessie, M., Fentie, D., Deckers, J., Frankl, A., Poesen, J., Adgo, E., & Nyssen, J. (2018). Revisiting lake sediment budgets: How the calculation of lake lifetime is strongly data and method dependent. *Earth Surface Processes and Landforms*, 43(3), 593–607. https://doi.org/10.1002/esp.4256

Leta, M. K., Waseem, M., Rehman, K., & Tränckner, J. (2023). Sediment yield estimation and evaluating the best management practices in Nashe watershed, Blue Nile basin, Ethiopia. *Environmental Monitoring and Assessment*, 195(6), 716. https://doi.org/10.1007/s10661-023-11337-z

Menberu, Z., Mogesse, B., & Reddythota, D. (2021). Assessment of morphometric changes in Lake Hawassa by using surface and bathymetric maps. *Journal of Hydrology: Regional Studies*, 36, 100852. https://doi.org/10.1016/j.ejrh.2021.100852

Meusburger, K., Steel, A., Panagos, P., Montanarella, L., & Alewell, C. (2012). Spatial and temporal variability of rainfall erosivity factor for Switzerland. *Hydrology and Earth System Sciences*, 16(1), 167–177. https://doi.org/10.5194/hess-16-167-2012

Moges, A., & Holden, N. M. (2007). Effects of wildfire, salvage logging and slash. *Land Degradation & Development*, 607, 591–607. https://doi.org/10.1002/ldr

Moges, A., & Holden, N. M. (2008). Estimating the rate and consequences of gully development: A case study of Umbulo catchement in southern Ethiopia. *Land Degradation & Development*, 19(5), 574–586. https://doi.org/10.1002/ldr

Molla, T., & Sisheber, B. (2017). Estimating soil erosion risk and evaluating erosion control measures for soil conservation planning at Koga watershed in the highlands of Ethiopia. *Solid Earth*, 8(1), 13–25. https://doi.org/10.5194/se-8-13-2017

Moore, I., & Burch, G. J. (1986). Division S-6-soil and water management physical basis of the length-slope factor in the universal soil loss equation 1. *Soil Conservation*, 50, 1294–1298.

Mtibaa, S., Hotta, N., & Irie, M. (2018). Analysis of the efficacy and cost-effectiveness of best management practices for controlling sediment yield: A case study of the Joumine watershed, Tunisia. *Science of the Total Environment*, 616–617, 1–16. https://doi.org/10.1016/j.scitotenv.2017.10.290

Mutua, B. M., & Klik, A. (2006). Estimating spatial sediment delivery ratio on a large rural catchment. *Journal of Spatial Hydrology*, 6(1), 64–80.

Neitsch, S., Arnold, J., Kiniry, J., & Williams, J. (2009). *Soil & water assessment tool theoretical documentation version* (pp. 1–647). Texas Water Resources Institute. https://doi.org/10.1016/j.scitotenv.2015.11.063

Nyesheja, E. M., Chen, X., El-Tantawi, A. M., Karamage, F., Mupenzi, C., & Nsengiyumva, J. B. (2019). Soil erosion assessment using RUSLE model in the Congo Nile Ridge region of Rwanda. *Physical Geography*, 40(4), 339–360. https://doi.org/10.1080/02723646.2018.1541706

Onyando, J. O., Kisoyan, P., & Chemelil, M. C. (2005). Estimation of potential soil erosion for river Perkerra catchment in Kenya. *Water Resources Management*, 19(2), 133–143. https://doi.org/10.1007/s11269-005-2706-5

Ouyang, D., & Bartholic, J. (1997). *Predicting sediment delivery ratio in Saginaw Bay watershed* (pp. 1–11). Institute of Water Research, Michigan State University.

Panditharathne, D. L. D., Abeysingha, N. S., Nirmanee, K. G. S., & Mallawatantri, A. (2019). Application of revised universal soil loss equation (RUSLE) model to assess soil erosion in "Kalu Ganga" River basin in Sri Lanka. *Applied and Environmental Soil Science*, 2019(1), 4037379. https://doi.org/10.1155/2019/4037379

Phinzi, K., & Ngetar, N. S. (2019). Land use/land cover dynamics and soil erosion in the Umzintlava catchment (T32E), Eastern Cape, South Africa. *Transactions of the Royal Society of South Africa*, 74(3), 223–237. https://doi.org/10.1080/0035919X.2019.1634652

Renard, K. G., Foster, G. R., Weesies, G. A., & Porter, J. P. (1991). RUSLE: Revised universal soil loss equation. *Journal of Soil and Water Conservation*, 46(1), 30–33.

Renard, K. G., Kimberlin, F. F., Moldenhauer, L. W., & William, C. (1997). *Predicting soil erosion by water: A guide to conservation planning with the revised universal soil loss equation (RUSLE)*. United States Government Printing.

Sabri, E. M., Boukdir, A., Meslouhi, R. E., Mahboul, A. E., Romaric, V., & Mbaki, E. (2017). Predicting soil erosion and sediment yield in Oued El Abid watershed, Morocco. *Athens Journal of Sciences*, 4(3), 225–242.

Thomas, J., Joseph, S., & Thrivikramji, K. P. (2018). Assessment of soil erosion in a monsoon-dominated mountain river basin in India using RUSLE-SDR and AHP. *Hydrological Sciences Journal*, 63(4), 542–560. https://doi.org/10.1080/02626667.2018.1429614

Tikuye, B. G., Rusnak, M., Manjunatha, B. R., & Jose, J. (2023). Land use and land cover change detection using the random forest approach: The case of the Upper Blue Nile River basin, Ethiopia. *Global Challenges*, 7(10), 1–11. https://doi.org/10.1002/gch2.202300155

Tsegaye, L., & Bharti, R. (2022). Soil erosion and sediment yield assessment using RUSLE and GIS-based approach in Anjeb watershed, Northwest Ethiopia. *SN Applied Sciences*, 3(5), 1–19. https://doi.org/10.1007/s42452-021-04564-x

Wagari, A., Case, A., & Catchment, F. (2024). RUSLE model based annual soil loss quantification for soil erosion protection: A case of Fincha catchment, Ethiopia. *Air, Soil and Water Research*, 14(1), 1–17. https://doi.org/10.1177/11786221211046234

Wang, B., Zheng, F., & Römkens, M. J. M. (2013). Comparison of soil erodibility factors in USLE, RUSLE2, EPIC and Dg models based on a Chinese soil

erodibility database. *Acta Agriculturae Scandinavica. Section B. Soil and Plant Science*, 63(1), 69–79. https://doi.org/10.1080/09064710.2012.718358

Williams, J. R., & Berndt, H. D. (1977). Sediment yield prediction based on watershed hydrology. *Transactions of the American Society of Agricultural Engineers*, 20(6), 1100–1104. https://doi.org/10.13031/2013.35710

Wischmeier, W. H., & Smith, D. D. (1978). Rainfall energy and its relationship to soil loss. *Eos, Transactions, American Geophysical Union*, 39(2), 285–291. https://doi.org/10.1029/TR039i002p00285

Yesuph, A. Y., & Dagnew, A. B. (2019). Soil erosion mapping and severity analysis based on RUSLE model and local perception in the Beshillo catchment of the Blue Nile basin, Ethiopia. *Environmental Systems Research*, 8(1), 1–21. https://doi.org/10.1186/s40068-019-0145-1

Yusof, M. A. M., Razi, M. A. M., Daud, H. Z. H., Azhar, E. A. K., Rani, M. S. M., & Al-Gheethi, A. (2023). Sediment erosion and yield analysis on the coast of Kedah and Langkawi, Malaysia: A case study. IOP Conference Series: Earth and Environmental Science, 1205(1), 12025. https://doi.org/10.1088/1755-1315/1205/1/012025

Zerihun, M., Mohammedyasin, M. S., Sewnet, D., Adem, A. A., & Lakew, M. (2018). Assessment of soil erosion using RUSLE, GIS and remote sensing in NW Ethiopia. *Geoderma Regional*, 12, 83–90. https://doi.org/10.1016/j.geodrs.2018.01.002

Zhang, S., Liu, Y., & Wang, T. (2014). How land use change contributes to reducing soil erosion in the Jialing River Basin, China. *Agricultural Water Management*, 133, 65–73. https://doi.org/10.1016/j.agwat.2013.10.016